SimBuild
2024

Eleventh National Conference of IBPSA-USA
Denver, Colorado
May 21 – 23, 2024

Augmenting Thermal Mass Performance without Added Carbon Footprint: Surface Area Modulation of Structural Slabs in Naturally Ventilated Buildings

Zherui Wang[1], Xiang Zhang[1], Xiaoxiao Peng[1], Saeran Vasanthakumar[2] and Dorit Aviv[1]
[1]University of Pennsylvania Weitzman School of Design, Philadelphia, PA, USA
[2]Autodesk, Toronto, ON, Canada

Abstract

Internal thermal mass (ITM) is a well-known passive technique that provides lag and damping for extreme diurnal temperature fluctuations when combined with natural ventilation and night flushing. Thermally massive concrete slab elements, vital for ITM, often feature a compact solid design, limiting their thermal storage potential due to restricted contact with indoor airflow. With the advent of architectural geometry and digital fabrication, floor elements can be designed and fabricated with greater exposed surface area under the constraint of the same material volume, thus maintaining the same embodied carbon footprint, but increasing its thermal performance potential. This study examines the impact of increasing exposed surface area of ITM through geometric modulation while keeping the material volume constant to reduce the building's embodied carbon. The objective is to investigate how varying ITM surface area, within a fixed material volume constraint, influences the indoor thermal comfort in a free-running building. We examine a case study of a midsize office building in two climatic zones (Tucson, AZ and San Diego, CA) with an increased ITM ceiling surface area of the structural slab. We then apply natural ventilation optimization and night flushing to further increase the ITM performance. The results show that in the hot-dry and marine climates expanding ITM surface area by 1.7 times yields improvement of 6% and 7% annual thermal comfort hours when coupled with natural ventilation. These findings suggest a substantial energy-saving potential for enlarging the surface area of ITM in buildings within the studied climates.

Introduction

The thermal absorption, storage, and release capacities of building materials can be used to reduce operational energy, and heating and cooling loads. Using adequate internal thermal mass (ITM) in buildings is generally regarded as an efficient solution for 'climate responsive architectural design' and 'passive solar design' (Givoni 1992; Shaviv, Yezioro, and Capeluto 2001), since it can mitigate the fluctuations of indoor thermal dynamics (e.g., indoor air temperature) (Gagliano et al. 2014), improving the thermal comfort of occupants for free-running buildings and reducing the energy consumptions for buildings with active systems (i.e., HVAC). Specifically, thermal masses 'provide both a dampening and a delaying effect on internal temperature' that can contribute to load reduction, energy saving, and improved thermal comfort (Li and Malkawi 2016). However, 'thermal mass is not always beneficial to comfort and energy consumption'(Verbeke and Audenaert 2018). For example, a longer time is generally required to reach the cooling or heating set point temperatures in buildings equipped with a large amount of thermal mass, which might lead to thermal discomfort of occupants and increase building energy consumption attributed to longer pre-heating or pre-cooling hours (Karlsson, Wadsö, and Öberg 2013). Therefore, quantifying the suitable amount of effective thermal mass for a specific climatic condition is needed (Slee, Parkinson, and Hyde 2014; Yam, Li, and Zheng 2003).

The effectiveness of thermal mass is co-determined by the functioning of transient heat conduction and storage, surface convection, and temperature-driven airflow. Thermal conductivity and diffusivity are key in understanding thermal mass property and performance. Diffusivity measures the ratio between thermal storage and thermal transmittance of a material due to temperature difference. For a given conductivity, lower the diffusivity, higher the specific heat capacity and density. The relationship between conductivity and diffusivity of a material can be described as

$$a = k/\rho Cp, \qquad (1)$$

where a is diffusivity (-), k thermal conductivity (W/mK), ρ density (kg/m³), and Cp Specific heat (J/kgK) of the material. Heat storage and surface convection are predominantly dependent on the volume of the mass and its effective surface area exposure for air change. These key factors have been characterized analytically by Holford and Woods (2007) and Craig (2019) as mathematical ratios to synchronize natural ventilation with surface area, mass thickness, and thermal properties of the mass material. With analytical models, Craig (2019) demonstrated that it is feasible in a single thermal zone building to achieve the damping and delay effect of ITM by expanding surface area exposure without increasing its corresponding material volume.

Maintaining the volume of the mass minimizes carbon footprint generally associated with ITM materials, and offers the additional benefit of carbon emission reduction without hindering ITM performance. For these reasons, identifying the effect of surface area exposure independent from its volume for ITM in buildings is important, particularly in the context of assessing the effect of ITM on operational energy and indoor thermal comfort of the occupants. However, existing studies tend to focus on quantifying the combined influence of volume and surface area of ITM, rather than investigating the influence of effective ITM surface area independent from its material volume. For example, Nelson and Henze (2021) conducted a parametric study on the relationship between concrete floor slab depth (between 0.1 cm and 30 cm) and operational energy consumption for an office building in six climate zones (2A, 3A, 3C, 4C, 5B and 6B). Their study revealed that increasing the ITM depth up to 7.5 cm to 10 cm can add additional operational energy saving on cooling across studied climate zones. In this case, the effective surface area exposure remains unchanged, while adding ITM thickness to increase the corresponding material volume, thereby augmenting ITM performance while simultaneously increasing carbon footprint.

In recent years, although some studies (Friedman 2015; Fortin and Craig 2021) have investigated geometrically activated ITM to maximize natural surface convection, the emphasis has been placed on exploring the building component scale rather than examining the impacts of increased effective exposed surface area of ITM for the entire building. To address this gap in the literature, we aim to investigate the potential of geometrically modulated ITM with an expanded surface area to passively enhance indoor thermal comfort at the whole building scale, and to compare its performance with the conventional flat ITM with an equivalent material volume. To the best of the authors' knowledge, using whole building energy simulation to assess the dynamic behavior of ITM with detailed geometries has not been studied in the literature at the time of preparing this article.

In addition, with the advent of advanced robotic manufacturing and 3D printing, producing geometrically complex and modulated components in building construction, such as facades (Leschok et al. 2023) and floor systems (Menna et al. 2020) has become increasingly feasible. These modulated building components can be robotically fabricated with thermally massive building materials (e.g., concrete) and function as ITM. In contrast to the conventional flat structural slabs, the geometric modulation afforded by advanced fabrication techniques allows ITM to be constructed with a greater control of the exposed surface area and material volume. The fabrication feasibility enables a broader applicability of the decoupling of ITM volume and surface area in practice, and ultimately unlocks the potential to augment ITM performance without added carbon footprint.

Case Study

This study examines the performance of a 3D-printed concrete structural element. The floor element is designed with minimized material volume for efficient structural and material life cycle consideration, and with maximized surface area for expanded thermal storage and carbon capture potential.

As a preliminary study, the Department of Energy (DoE) Medium Office Building is used as the baseline and simulated under the free-running scenario. The International Energy Conservation Code (IECC) U.S. climate 2B (hot-dry in Tucson) and 3C (marine in San Diego) climate zones are selected as the outdoor climatic condition, given its reported ITM benefit for building energy reduction (Reilly and Kinnane 2017). The hot-dry climate of Tucson, AZ is selected because of the significant diurnal temperature swing and known optimal thermal mass performance with the conventional flat ITM ceiling surface configuration (Nelson and Henze 2021). The marine climate of San Diego, CA is chosen as a comparison for its milder climate and most potential for operational energy reduction (Ghattas, Ulm, and Ledwith 2013). Typical meteorological year (TMY3) EnergyPlus Weather files (USA_AZ_Tucson-Davis-Monthan.AFB.722745_TMY3 for 2B Tucson, Arizona, and USA_CA_San.Deigo-Brown.Field.Muni.AP.722904_TMY3 for 3C San Diego, California) provided by the US Department of Energy reference building dataset are used as weather data for the simulations.

Natural ventilation and night flushing are deployed in this study. Figure 1 illustrates a second-floor thermal zone with flat ITM ceiling surface versus shaped surface with expanded surface area colored in magenta. Table 1 details the construction sets and geometric properties of the ceiling Zone Surface in the baseline, flat, and shaped scenarios. The analysis focuses on the second-floor zones to limit the roof and ground temperature influence to the indoor temperature dynamics.

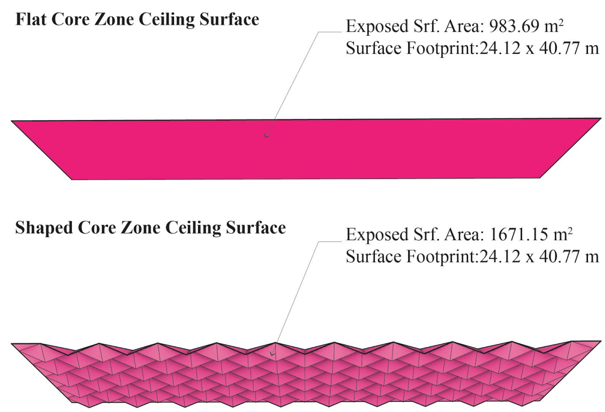

Figure 1: Geometric manipulation of the thermal zone ceiling surface to achieve expanded surface area with the same footprint. A reflected view of the ceiling surfaces looking from below is shown.

Table 1 thermal and geometric properties of ceiling/floor surface construction

	Baseline Ceiling Surface Construction	Flat ITM Ceiling Surface Construction	Shaped ITM Ceiling Surface Construction
Material	Acoustic tile	Concrete	
Thickness [m]	0.0127	0.05	0.03
Material Surface Area [m^2]	1660.73	1660.73	2777.88
Material Volume [m^3]	21.09	83.34	
Conductivity [W/mK]	0.0576	2.31	
Density [kg/m^3]	288.332	2322	
Specific heat [J/(kg K)]	795.492	832	
Roughness	Medium Smooth		

Methods

Building Energy Modeling Workflow

This section provides a description of the proposed building energy modeling (BEM) workflow to evaluate thermally massive floor elements with expanded surface area exposure. Figure 2 shows the BEM geometries with flat ITM versus with shaped ITM.

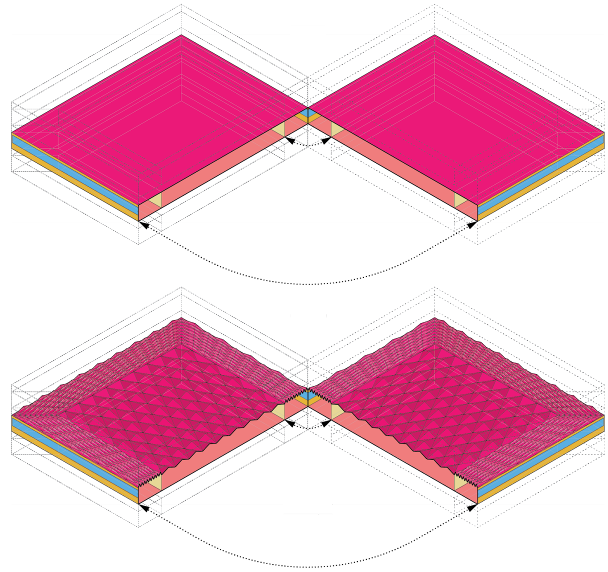

Figure 2: Building energy modeling geometry unfolded in section. The second floor zones are highlighted showing the a) flat ITM ceiling surface, and b) shaped ITM ceiling surface in magenta.

Modeling complex, detailed geometry is still a challenge in BEM environments like EnergyPlus and OpenStudio. While it is a common practice to simplify thermal zone geometry to the least number of surfaces, this approach expands the performance gap. Some authors have reported that geometry details can increase building energy simulation reliability for up to 15% (Isaacs et al. 2014), while others have shown that a range of 15.7% to 95.2% simplification of a complex building envelope geometry results in 0.6% to 11.4% errors on end-use energy (Santos, Schleicher, and Caldas 2019).

To account for the expanded surface area characteristics of the model, we construct the BEM geometry in Rhinoceros to take advantage of its versatility in modeling detailed geometry representative of the floor element. To facilitate a streamlined translation between detailed geometry and BEM, we use Ladybug Tools (LBT) for Grasshopper to assign associated construction sets, programs, and additional energy modeling parameters. Significant discrepancies exist between the complex and detailed DoE Medium Office Building and the standard LBT energy modeling, since LBT default assumptions are more suitable for simpler energy models. To address this modeling gap, we devise customized LBT models by modifying a series of energy parameters that are typically left unmodified. Additionally, LBT only implements a subset of EnergyPlus objects within the standard toolset, resulting in most detailed DoE reference parameters being inaccessible in standard LBT. Therefore, additional considerable efforts have been made to customize the LBT model in this study. For instance, the standard LBT oversimplifies the impacts of ground temperature. To narrow the gap between LBT and real-world conditions, the dynamic monthly ground temperatures are pre-simulated and assigned in the customized LBT.

Additional LBT limitations include a single HVAC loop assigned for the entire building; simplified mixed water heater volume and demand; simplified lighting sensor, control, and load calculation; different methods in generating .ddy files; and many others – all of which contribute to the inconsistent modeling results. To reconcile the difference, we reference the OpenStudio measure in the Building Component Library to generate a baseline idf file and use custom python components in Grasshopper to swap and update default objects to baseline Medium-sized Office Building equivalence. This groundwork allows us to streamline the parametric workflow for assessing ITM performance of the building fabric in future studies.

Thermal Mass Modeling with Geometric Representation

Typically, ITM can be modeled either via Internal Mass object or as part of the Zone Surface in EnergyPlus. With the Internal Mass object method, additional surface area and material volume of the shaped ITM can be accounted for in addition to the flat ITM surface area and volume modeled via Zone Surfaces. However, the Internal Mass object assumes lumped material properties and factored over the floor area of a thermal zone. While the indoor heat balance of Internal Mass accounts for surface temperature and factors in its effect on indoor air temperature, Internal Mass objects do not participate in indoor shortwave and longwave radiant heat exchange with surrounding surfaces (U.S. Department of Energy 2022). This simplification may be a direct consequence of the lack of geometric representation.

Another method to account for ITM in EnergyPlus is to have thermally massive materials (i.e. concrete) built into the construction set of the Zone Surface. In this case, the Zone Surface participates in shortwave radiation from solar and internal sources, longwave radiation exchange with adjacent surfaces in the zone and internal sources, conduction from both sides of the surface, and convective heat exchange with zone air. The thermal absorption and dissipation of ITM through conduction is calculated by the Conduction Transfer Function Modules. The convective heat exchange between the Zone Surface and the indoor air is modeled with the Surface Convection Algorithm. Specifically, the TARP (Thermal Analysis Research Program) model algorithm is applied consistent with the US Department of Energy prototype building models. The TARP model correlates convective heat transfer coefficient to surface orientation and temperature difference based on experimentally collected data. Modeling ITM with this Zone Surface based approach allows geometric representation crucial to the shaped ITM and a more complete account for all modes of indoor thermal dynamics.

Floor Element Surface Characteristics

After generating the baseline BEM, our approach models the expanded surface area exposed to air as Zone Surface, where the EnergyPlus Inside Heat Balance Method considers conduction through the surface, convection to the air, short and long wave radiation absorption, reflectance and interchange. The actual 3D-printed concrete floor element we reference in the literature (Anton et al. 2023) is highly detailed with cavity and surface twists that are challenging to capture within the BEM environment. To ensure computational and modeling feasibility, the ceiling surfaces of each thermal zone are isolated and tessellated into 2-directional folded plates (Figure 1). In this manner, the geometric manipulation through tessellation allows expanded surface area without enlarging its footprint, ensuring that the same thermal zone volume can be enclosed. This strategy approximates the 3D-printed concrete floor element with matching exposed surface area, material volume, surface orientation, thickness, and overall shape. Thus, simulation errors induced by the surface shaped factor can be accounted for and minimized.

Natural Ventilation Control Strategies

To maximize the ITM cooling performance potential, natural ventilation is simulated through the EnergyPlus Airflow Network. Operable windows are assumed to be horizontally sliding windows with 50% operable area, and the discharge coefficient is set to be 0.45 for unobstructed aperture with insect screen. No wind-driven cross ventilation is assumed given the single-sided nature of the window placement. While the core zone does not have direct window access, the interzone surfaces are not adiabatic and subjugates heat and air exchange with the perimeter zones.

With an Energy Management System (EMS) program, the operable windows are dynamically controlled based on the desired minimum and maximum indoor and outdoor temperatures or delta temperature between indoor and outdoor. A total of 324 minimum and maximum temperature combinations are iteratively tested on a 1°C increment. 30 additional iterations with a 0.5°C increment on the delta and minimum inside temperature combinations is subsequently tested on the baseline Medium-sized Office Building, to identify the most optimal indoor condition based on the comfort hours obtained from the adaptive comfort model. As mentioned in the case study section, this workflow is applied to both Tucson and San Diego climate zones.

In the context of Tucson's cooling dominant climate, the Medium-sized Office Building's core and perimeter thermal zones exhibit varying degrees of exposure to diurnal ambient temperature swings and natural ventilation access. As a result, optimal tuning strategy of natural ventilation control temperatures for these zones may differ to prevent overheating of the core zone, which may result in suboptimal comfort hours on the perimeter zones, and vice versa. Given that the layout characteristic of the study case is dominated by the core zone area (Figure 2), applying the weighted area averaging of five zones might overlook the thermal comforts in perimeter zones. Therefore, in this study, the average comfort hours under different natural ventilation control strategies are calculated directly via simple arithmetic mean of the thermal comfort hours in the said five zones. Table 2 summarizes the top ranking candidates of optimal ventilation control strategies to maximize averaged comfort hours in five thermal zones on the second floor. In addition, setting minimum indoor air and delta temperatures as 21°C and 0.5°C respectively can contribute to the maximized hours of thermal comfort on the second building floor (Figure 3). For San Diego, the same workflow is applied, and the optimized minimum indoor air and delta temperatures amount to 20.5°C and 0.5°C respectively. These natural ventilation control strategies serve as the input setting for the subsequent comparison of thermal comfort performances under two scenarios of ceiling surface visualized in Figure 2.

Table 2: Top ranking natural ventilation control strategies for Tucson, AZ.

Rank	Min. Indoor air Temperature (°C)	Delta Temperature (°C)	Average Comfort Hours for Five Zones (hours)
1	21	0.5	2103.5
2	21	1	2088.7
3	21.5	0.5	2078.8
4	21.5	1	2064.6
5	21	1.5	2060.4
6	22	0.5	2057.7
7	20.5	0.5	2051.4

Note: The total annual operational hours from 6 a.m. to 9 p.m. are 4836 hours, holidays and Sundays excluded.

Night Flushing and Window Open Control Strategies

Given the occupancy schedule of the medium-size office building, the unoccupied overnight hours are not constrained to the tight temperature band required for the occupied hours, and bear potential for additional cooling storage. To assess the maximum effect of night flushing on the indoor air temperature and occupant comfort, we identify selective days to apply night flushing during unoccupied hours on top of the optimized, rule-based natural ventilation control. Three sequential days within the year are identified based on two criteria – large diurnal outdoor air temperature swing and the peak over 30°C. April 21st to 23rd in Tucson and October 14th to 16th in San Diego are identified as days with larger than 17°C diurnal temperature difference to assess the peak indoor air temperature reduction and adaptive comfort improvement between the flat and shaped ITM elements.

Customized window control schedule is devised and optimized for each of the selected days. The objective of the schedule optimization is to maximize daytime peak temperature reduction (and by extension adaptive comfort hours) while minimizing over cooling in the occupied early morning hours. Currently, the window operation schedule is controlled hourly based on the hourly resolution of the TMY data. This can be modified with sub-hour resolution in future work. With 8-hour unoccupied hours overnight on a typical workday, there are 256 unique combinations for the window being open or closed. To further reduce high computational cost associated with simulating detailed BEM geometries, 16 combinations of consecutive window opening hours are tested for each thermal zone. The same optimization solution selection criteria to that of the hourly natural ventilation control (i.e., the highest adaptive comfort percentage) is applied to identify the optimal window opening schedule overnight.

Adaptive Comfort Assessment

The Adaptive Thermal Comfort (ASHRAE Standard 55) is used to assess the impact of the exposed concrete ceiling surface on occupant thermal comfort over 4836 annual occupied hours for each thermal zone on the second floor. The comfort model accounts for the mean indoor air temperature, mean radiant temperature (MRT), relative humidity, airspeed, metabolic rate, and clothing value of the occupants. The MRT is derived from the EnergyPlus Zone Mean Radiant Temperature output, which uses the weighted average of surface area multiplied by emissivity of the thermal zone inside surface temperatures. The top ranked natural ventilation control strategy is deployed to obtain the best adaptive comfort hour and percentages achieved. The number of added comfort hours between the models with flat and shaped ITM ceiling surfaces are compared with the baseline Mid-Office building. The second-floor zones are used to limit the roof and ground temperature influence.

Results

This section is divided into three parts: first, the annual adaptive comfort improvement with shaped ITM for Tucson and San Diego climate profiles; second, analysis on the indoor air temperature and MRT over the course of the day for two months with the most comfort improvement in Tucson; and third, comparison of the adaptive thermal comfort, indoor air temperature, and convective heat transfer coefficient between the scenarios with hourly natural ventilation control and that with added night flushing on selected three-day periods in Tucson and San Diego.

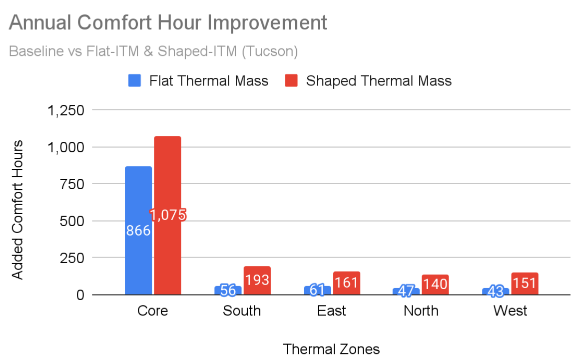

a)

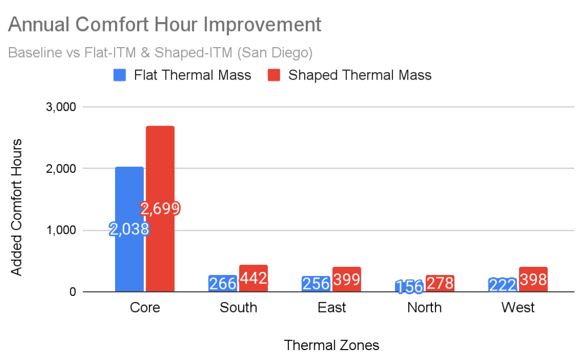

b)

Figure 3: Annual added comfort hour from the baseline for flat and shaped ITM in a) Tucson and b) San Diego.

Adaptive Thermal Comfort Assessment: Flat and Shaped Ceiling Surfaces

Adding ITM to the ceiling of each thermal zone shows immediate adaptive thermal comfort improvement from the Medium-sized Office Building baseline, particularly with shaped thermal mass. In Tucson, using shaped ITM elements results in additional 1075 annual comfort hours in the core zones compared to the baseline model with acoustic ceiling tiles. Similar improvements are observed in south, east, west, and north zones with 193, 161, 140, and 151 additional hours compared to the baseline (Figure 3.a). Substantial improvements are observed from November to April across five zones, as shown in Figure 4.a. Similarly, in San Diego climate, considerable annual comfort hours are added (Figure 3.b), amounting to 2699, 442, 399, 278, and 398 hours in the core, south, east, west, and north zones. The months of July to September exhibit the highest monthly improvement between flat and shaped ITM models (Figure 4.b). The core zone experiences the most significant annual comfort improvement induced by the geometric modulation of the ITM. Across the year, there is a minimal reduction in comfort hours compared to the baseline for both climates between flat and shaped ITM models.

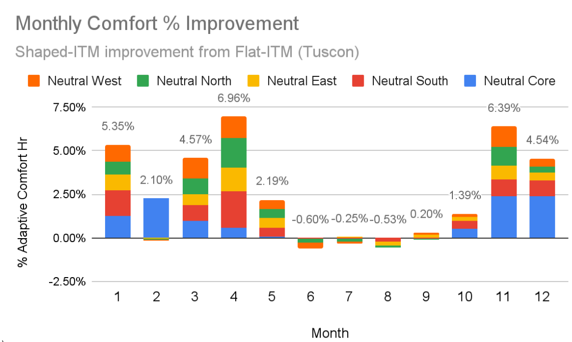

a)

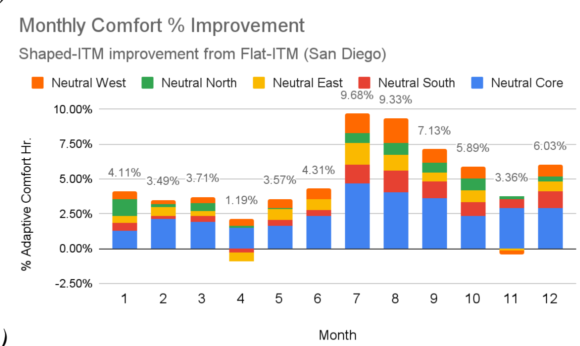

b)

Figure 4: Monthly adaptive comfort (neutral) hour percentage improvement from flat to shaped ITM ceiling surfaces across thermal zones for a) Tucson and b) San Diego.

Indoor Air Temperature and Mean Radiant Temperature Assessment of the Internal Thermal Mass Performance: Flat and Shaped Ceiling Surfaces

To further investigate why and how geometrically shaped ITM outperforms traditional flat ITM (Figure 2), based on the selected data, Figures 5-6 illustrate how shaped ITM can better dampen indoor air temperature and MRT than flat ITM under the same conditions with natural ventilation.

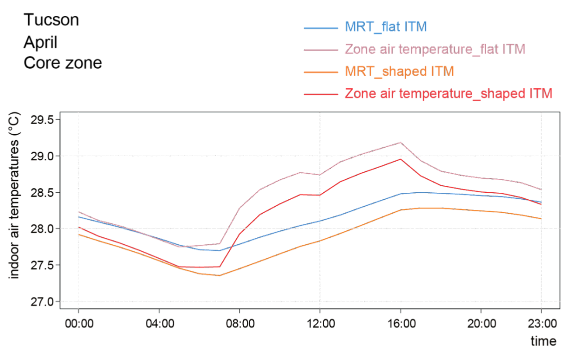

a)

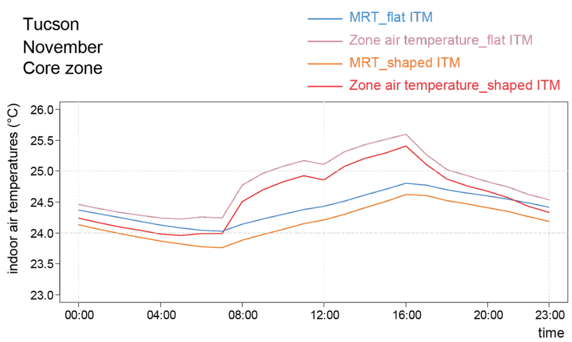

b)

Figure 5: Monthly average daily indoor air temperature and MRT profiles in the core zone comparing the flat and shaped ITM models in a) April, and b) November at Tucson.

Using the two months with highest comfort hour improvement in Tucson as an example, we observe a general reduction and a slower hourly change in both indoor air temperature and MRT in perimeter and core thermal zones. In April, the shaped ITM is able to reduce core zone indoor air temperature from 0.19°C to 0.35°C, and MRT from 0.21°C to 0.34°C on average over the course of the day (Figure 5a). Similar trends are observed in November with 0.15°C to 0.27°C reduction on indoor air temperature and 0.17°C to 0.26°C on MRT (Figure 5b). In May, the indoor air temperature and MRT show similar peak reduction at 0.36°C and 0.34°C respectively. However, the temperature reduction ranges are already outside of the adaptive thermal comfort band, and render limited comfort improvement. In general, the core zone shows consistent temperature reductions across the year. The ITM volume and surface area exposure afford greater degree of damping to the core zone dominated by the internal thermal load.

In the south-facing perimeter zone, the shaped ITM reduces the peak indoor air temperature by 0.7°C and MRT 0.76°C in April (Figure 6a), and by 0.35°C and 0.77°C respectively in November (Figure 6b). In May, while there is a similar reduction in peak indoor air temperature at 0.66°C and MRT at 0.63°C, achieving thermal comfort with shaped ITM alone becomes challenging given the rising heating load of the month.

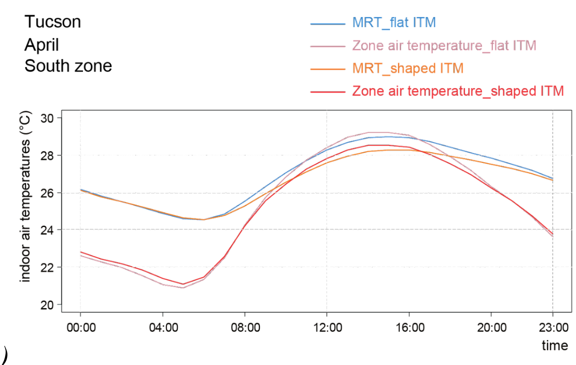

a)

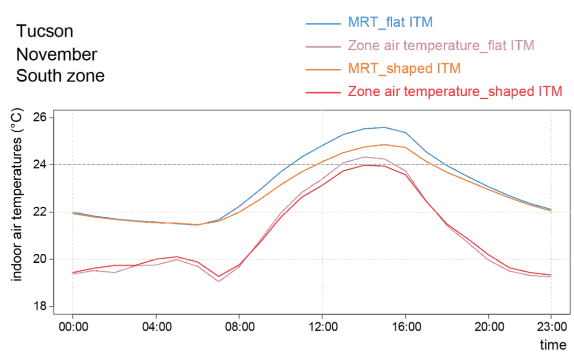

b)

Figure 6: Monthly averaged daily indoor air temperature and MRT profiles in the south zone comparing the flat and shaped ITM models in a) April, and b) November at Tucson.

Assessment of the Internal Thermal Mass Performance Assisted by Night Flushing: Flat and Shaped Ceiling Surfaces

Adding night flushing during unoccupied hours on top of optimized, rule-based natural ventilation control results in a decrease in peak indoor air temperatures in both Tucson and San Diego, as shown in Table 3. The south zone is used as an example herein.

Table 3: The peak indoor air temperature of the south zone averaged across the 3 selected days for flat and shaped ITM models with and without night flushing in Tucson (April 21st to 23rd) and San Diego (October 14th to 16th).

Thermal Mass and Natural Ventilation Scenarios	Tucson, AZ	San Diego, CA
Flat ITM with Hourly Natural Ventilation Control	28.48°C	30.57°C
Shaped ITM with Hourly Natural Ventilation Control	27.66°C	29.56°C
Shaped ITM with Hourly Natural Ventilation Control and Night Flushing Applied	26.67°C	28.15°C

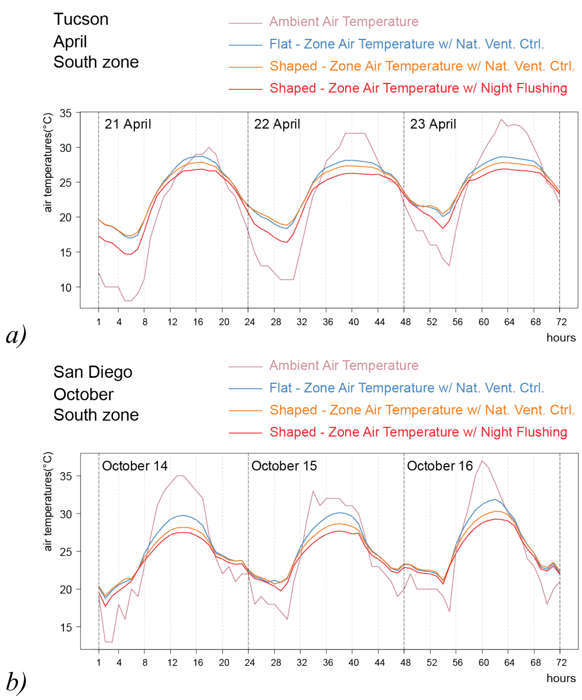

Figure 7: Daily outdoor and indoor air temperature profiles in the south zone comparing between the flat and shaped ITM with hourly natural ventilation control and that with added night flushing. Scenarios in a) Tucson on selected April days, and b) San Diego on selected October days are shown.

In Tucson, with night flushing, the flat ITM model enjoys a peak temperature reduction of 1.03°C on average across the 3 selected days, and the shaped ITM 0.99°C (Figure 7a). Between the flat ITM with hourly natural ventilation control and the shaped ITM with night flushing applied, a total of 1.81°C peak temperature reduction is observed. By introducing shaped ITM, 75% to 100% of the overheating hours observed in the flat ITM model are removed. Adding night flushing fully mitigates daytime overheating. With shaped ITM, interior space may be over-cooled from 5 am to 7 am; however, these hours see a considerably lower occupancy rate from 10 to 20%. Table 4 illustrates the adaptive comfort hour percentage for the selected days for flat and shaped ITM models with hourly natural ventilation control and added night flushing. Similarly in San Diego, the 3-day averaged daily peak indoor air temperature reduces by 1.54°C in the flat ITM model, and 1.41°C in the shaped ITM model (Table 3). Applying night flushing and introducing shaped ITM consistently reduces daytime peak indoor air temperature (Figure 7b) and overheating hours.

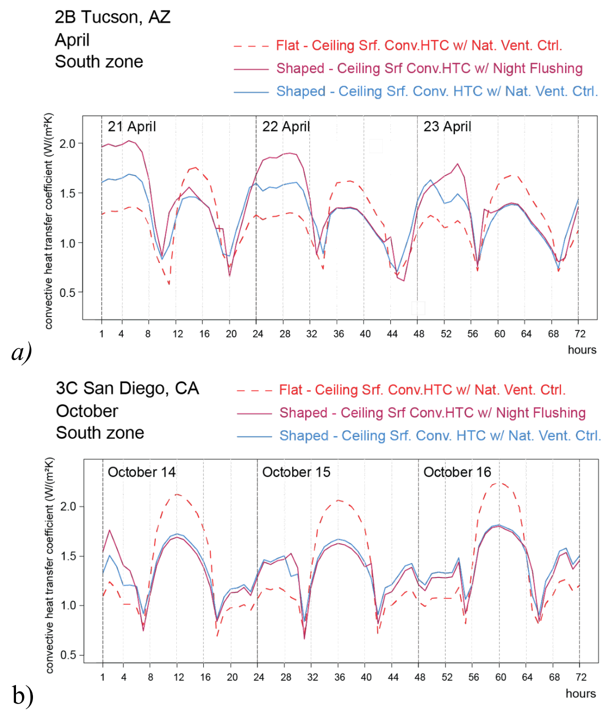

Figure 8: Convective heat transfer coefficient of the ceiling surface in the south zone comparing between the flat and shaped ITM with hourly natural ventilation control and that with added night flushing. Scenarios in a) Tucson on selected April days, and b) San Diego on selected October days are shown.

Table 4: The adaptive comfort percentage of the south zone for flat and shaped ITM models with and without night flushing on selected days in Tucson (April 21st to 23rd) and San Diego (October 14th to 16th).

Thermal Mass and Natural Ventilation Scenarios	Tucson, AZ	San Diego, CA
Flat ITM with Hourly Natural Ventilation Control	41.67%	37.50%
Shaped ITM with Hourly Natural Ventilation Control	79.17%	41.67%
Shaped ITM with Hourly Natural Ventilation Control and Night Flushing Applied	77.08%	52.08%

Discussion

The annual adaptive comfort results demonstrate significant improvements in both added comfort hours and monthly comfort percentage (Figures 3 to 4), aligned with the indoor temperature-damping effect of the thermal mass (Figures 5 to 6). This observed difference may be attributed to multiple factors. Primarily, the reduction in indoor surface temperature, and by extension lowered MRT within the thermal zone, plays a role in enhancing occupant thermal comfort. During occupied hours, typically ranging from 6:00 to 21:00, MRT curves consistently indicate lower values compared to indoor air temperature across both core and south zones. Notably, in the shaped ITM scenario, both indoor air temperature and MRT display visibly slower rates of change due to the ITM effect. This observed trend aligns with the preferences of the adaptive comfort model, which tends to favor conditions characterized by gradual temperature changes over time rather than abrupt fluctuations.

Furthermore, the adaptive comfort model has different sensitivity to air velocity above and below 24°C. When the air temperature is higher than 24°C, the upper comfort boundary of the comfort range may widen, particularly during cooling dominant hours. In such cases, indoor air temperature alone may not serve as the predominant parameter governing adaptive occupant comfort. Therefore, the combination of these factors likely contributes to the differences observed between the increased thermal comfort hours and the lesser degree of indoor air temperature damping between the flat and shaped ITM scenarios. Additional investigations are required for future research.

We observe that shaped ITM with hourly natural ventilation control can achieve similar or better adaptive comfort hours compared to flat ITM in Tucson and San Diego. This is attained with geometric modulation of expanded surface area exposed to air and surface orientation alone, while the material volume remains unchanged. Furthermore, the shaped ITM model has the potential to gain additional comfort hours when the night flushing schedules are systematically optimized. Consequently, with an optimized natural ventilation control strategy and night flushing, geometric modulation of ITM elements can improve comfort with the same embodied carbon footprint considering the overall material volume.

Further, across both Tucson and San Diego climates, the increase in adaptive comfort hours with expanded ITM surface exposure suggests reduced dependence on mechanical cooling and heating, highlighting the potential for operational energy reduction. This underscores the importance of further research into optimizing HVAC system control alongside shaped ITM in the future.

Conclusion

In this study, we develop a modeling strategy to perform whole building energy simulation with specified geometric building elements. This approach allows us to investigate the effect of increasing the surface area of internal thermal mass (ITM) without increasing the material volume of the mass. The shaped ITM in our energy model is devised by geometrically shaping the ceiling surface through surface tessellation. This modulated surface configuration leads to a 65% increase in the exposed ITM surface area, while keeping the ITM volume constant. The simulation results presented in this study demonstrate improved indoor thermal comfort compared to the baseline model. Specifically, among all second-floor zones, we have observed an averaged addition of 130 hours and 256 comfort hours in Tucson and San Diego climates respectively.

Furthermore, the detailed indoor air temperature study conducted in two climate zones reveals that the surface geometry of the shaped ITM can be intelligently tuned to match the desired thermal performance based on factors such as load schedule, zone orientation, solar exposure, and climate conditions. Specifically, on the selected three-day study period, the expanded surface area exposure is shown to achieve improved convective heat transfer at the zone ceiling surface, allowing additional indoor air temperature damping and reducing the number of overheating hours.

With the assistance of night flushing, our study reveals that Tucson, AZ and San Diego, CA can achieve a substantial portion of comfort hours during the occupied periods with shaped ITM. Specifically, comfort hours ranging from 77% to 52% of total occupied hours were attained in these locations, compared to 42% and 37% achieved by their flat ITM counterparts. These results were observed on selected

October and April days characterized by significant diurnal temperature variations.

Using the DoE Medium Office Building as a case study, this paper opens up the investigation on deploying geometric design exploration to optimally tune the performance of thermal mass building elements for increased thermal comfort while minimizing carbon emissions associated with additional material usage. Future work will focus on integrating shaped ITM and HVAC systems with optimized control strategies and conducting subsequent operational and embodied energy assessments associated with whole building operation.

Acknowledgment

The authors acknowledge the support provided by the Advanced Research Projects Agency–Energy (ARPA-E) Grant of the U.S. Department of Energy (DE-AR0001631) to Dr. Masoud Akbarzadeh and Dr. Dorit Aviv.

References

Anton, Ana-Maria, Eleni Skevaki, Patrick Bischof, Lex Reiter, and Benjamin Dillenburger. 2023. "Column-Slab Interfaces for 3D Concrete Printing: Design, Fabrication and Assembly Strategies." In *Hybrids & Haecceities: Proceedings of the 42nd Annual Conference of the Association for Computer Aided Design in Architecture*, 58–59. Association for Computer Aided Design in Architecture. https://www.research-collection.ethz.ch/handle/20.500.11850/639150.

Craig, Salmaan. 2019. "The Optimal Tuning, within Carbon Limits, of Thermal Mass in Naturally Ventilated Buildings." *Building and Environment* 165 (November): 106373. https://doi.org/10.1016/j.buildenv.2019.106373.

Fortin, Remy, and Salmaan Craig. 2021. "Geometrically Activated Thermal Mass: Wood vs. Concrete." *Journal of Physics: Conference Series* 2042 (November): 012156. https://doi.org/10.1088/1742-6596/2042/1/012156.

Friedman, Jared. 2015. "Working Matter: Optimizing Material Distribution for Thermal Performance." Harvard University. https://jaredfriedman.org/Optimizing-Thermal-Mass.

Gagliano, A., F. Patania, F. Nocera, and C. Signorello. 2014. "Assessment of the Dynamic Thermal Performance of Massive Buildings." *Energy and Buildings* 72 (April): 361–70. https://doi.org/10.1016/j.enbuild.2013.12.060.

Ghattas, Randa, Franz-Joseph Ulm, and Alison Ledwith. 2013. "Mapping Thermal Mass Benefit." Cambridge, Mass.: Massachusetts Institute of Technology.

Givoni, Baruch. 1992. "Comfort, Climate Analysis and Building Design Guidelines." *Energy and Buildings* 18 (1): 11–23. https://doi.org/10.1016/0378-7788(92)90047-K.

Holford, J. M., and A. W. Woods. 2007. "On the Thermal Buffering of Naturally Ventilated Buildings through Internal Thermal Mass." *Journal of Fluid Mechanics* 580 (June): 3–29. https://doi.org/10.1017/S0022112007005320.

Isaacs, Nigel, Kay Saville-Smith, Michael Donn, Michael Camilleri, Andrew Pollard, Michael Babylon, Rob Bishop, et al. 2014. "Building Energy End-Use Study." Building Energy End-use Study (BEES) Part 1: Final Report 297/1,. Judgeford: BRANZ.

Karlsson, Jonathan, Lars Wadsö, and Mats Öberg. 2013. "A Conceptual Model That Simulates the Influence of Thermal Inertia in Building Structures." *Energy and Buildings* 60 (May): 146–51. https://doi.org/10.1016/j.enbuild.2013.01.017.

Leschok, Matthias, Ina Cheibas, Valeria Piccioni, Bharath Seshadri, Arno Schlüter, Fabio Gramazio, Matthias Kohler, and Benjamin Dillenburger. 2023. "3D Printing Facades: Design, Fabrication, and Assessment Methods." *Automation in Construction* 152 (August): 104918. https://doi.org/10.1016/j.autcon.2023.104918.

Li, Xiwang, and Ali Malkawi. 2016. "Multi-Objective Optimization for Thermal Mass Model Predictive Control in Small and Medium Size Commercial Buildings under Summer Weather Conditions." *Energy* 112 (October): 1194–1206. https://doi.org/10.1016/j.energy.2016.07.021.

Menna, Costantino, Jaime Mata-Falcón, Freek P. Bos, Gieljan Vantyghem, Liberato Ferrara, Domenico Asprone, Theo Salet, and Walter Kaufmann. 2020. "Opportunities and Challenges for Structural Engineering of Digitally Fabricated Concrete." *Cement and Concrete Research* 133 (July): 106079. https://doi.org/10.1016/j.cemconres.2020.106079.

Nelson, John, and Gregor Henze. 2021. "Evaluation of the Passive Cooling Potential of Thermal Mass Inherent in Medium to Large Commercial Buildings." *Journal of Architectural Engineering* 27 (2): 04021007. https://doi.org/10.1061/(ASCE)AE.1943-5568.000

0460.

Reilly, Aidan, and Oliver Kinnane. 2017. “The Impact of Thermal Mass on Building Energy Consumption.” *Applied Energy* 198 (July): 108–21. https://doi.org/10.1016/j.apenergy.2017.04.024.

Santos, Luis, Simon Schleicher, and Luisa Caldas. 2019. “Automatic Simplification Of Complex Building Geometry For Whole-Building Energy Simulations.” In *Proceedings of the 16th IBPSA Conference*, 2691–98. Rome, Italy: IBPSA. https://doi.org/10.26868/25222708.2019.210991.

Shaviv, Edna, Abraham Yezioro, and Isaac G Capeluto. 2001. “Thermal Mass and Night Ventilation as Passive Cooling Design Strategy.” *Renewable Energy* 24 (3): 445–52. https://doi.org/10.1016/S0960-1481(01)00027-1.

Slee, Ben, Tom Parkinson, and Richard Hyde. 2014. “Quantifying Useful Thermal Mass: How Much Thermal Mass Do You Need?” *Architectural Science Review* 57 (4): 271–85. https://doi.org/10.1080/00038628.2014.951312.

U.S. Department of Energy. 2022. “EnergyPlus™ Version 22.1.0 Documentation.” Engineering Reference. U.S. Department of Energy.

Verbeke, Stijn, and Amaryllis Audenaert. 2018. “Thermal Inertia in Buildings: A Review of Impacts across Climate and Building Use.” *Renewable and Sustainable Energy Reviews* 82 (February): 2300–2318. https://doi.org/10.1016/j.rser.2017.08.083.

Yam, Jimmy, Yuguo Li, and Zuohuan Zheng. 2003. “Nonlinear Coupling between Thermal Mass and Natural Ventilation in Buildings.” *International Journal of Heat and Mass Transfer* 46 (7): 1251–64. https://doi.org/10.1016/S0017-9310(02)00379-4.